Magnetic Nanowires

Cyanide-Bridged Iron(III)–Cobalt(II) Double Zigzag Ferromagnetic Chains: Two New Molecular Magnetic Nanowires[**]

Rodrigue Lescouëzec, Jacqueline Vaissermann, Catalina Ruiz-Pérez, Francesc Lloret, Rosa Carrasco, Miguel Julve, Michel Verdaguer,* Yves Dromzee, Dante Gatteschi, and Wolfgang Wernsdorfer*

The occurrence of a slow relaxation of the magnetization in a one-dimensional (1D) system was recently reported by one of us.[1] The system was claimed to illustrate, for the first time, a theoretical model designed by Glauber in 1963 for anisotropic Ising systems[2] and opened the perspective of a potential use of 1D magnetic molecular nanowires for information storage. Even though 1D magnetism is a very active area of research, such dynamic behavior was never detected before since it is not clear how to fulfill experimentally the requirements of a perfect 1D Ising-type chain. This finding prompted us to look carefully at 1D systems containing anisotropic elements, such as cobalt(II) and low-spin iron(III) centers that we synthesized recently,[3] to investigate their anisotropic magnetic properties and to study the dynamics of their magnetization.

The stable low-spin cyanide-containing iron(III) precursors $[Fe^{III}(L)(CN)_4]^-$ (L = bidentate nitrogen donor) react with hydrated metal ions in aqueous solution[4,5] and afford single crystals of the bimetallic double zigzag chains $[\{Fe^{III}(L)(CN)_4\}_2Co^{II}(H_2O)_2]\cdot 4H_2O$ (**1** with L = 2,2′-bipyridine (bpy) and **2** with L = 1,10-phenanthroline (phen)). We found that **1** and **2** show intrachain ferromagnetic coupling, 1D Ising-type behavior, slow relaxation of the magnetization, and hysteresis effects and thus are the second examples of anisotropic molecular magnetic nanowires and the first with an intrachain ferromagnetic coupling. Their preparation, X-ray crystal structure,[6] and preliminary static and dynamic magnetism are reported herein.

Compounds **1** and **2** are isostructural (monoclinic system, space group $P2_1/n$). They are made up of neutral cyanide-bridged Co^{II}–Fe^{III} double zigzag chains and uncoordinated water molecules which are linked through van der Waals forces and hydrogen bonds. Within each chain, the $[FeL(CN)_4]^-$ entity acts as a bismonodentate ligand towards two *trans*-diaquacobalt(II) units through two of its four cyanide groups in *cis* positions (Figure 1) affording bimetallic double chains which run parallel to the *a* axis (Figure 2). They show two orientations of their mean planes (Fe_2Co_2), forming an angle of ±70° with the *b* axis. The metal atoms in **1** and **2** are six-coordinate: two nitrogen atoms from bpy (**1**) or phen (**2**) and four cyanide carbon atoms around the Fe centers, two water molecules in *trans* position and four cyanide nitrogen atoms around the Co centers build distorted octahedral geometries. Bond lengths and angles around the Fe atom in **1** and **2** are close to those observed in the low-spin iron(III) unit $[FeL(CN)_4]^-$ (L = bpy and phen) in mononuclear,[4,5] heterotrinuclear,[5] and bimetallic chain[4,5] compounds. The values of the Fe-C-N angles for both terminal (176.3(3) and 176.7(2)° in **1** and 177.4(1) and 176.1(1)° in **2**) and bridging cyanides (174.6(2) and 178.7(2)° in **1** and 175.0(1) and 174.7(1)° in **2**) depart somewhat from strict linearity. The $Co–O_{water}$ bond (2.103(2) in **1** and 2.0886(4) Å in **2**) is similar to those observed in aqua complexes of high-spin cobalt(II).[7] The values of the $Co–N_{cyanide}$ bond lengths in **1** (2.125(2) and 2.104(2) Å) and **2** (2.147(2) and 2.113(2) Å) are significantly longer than those observed in the Co^{III}-N≡C-Fe^{III} unit (diamagnetic Co^{III} and low-spin Fe^{III}) of the single cyanide-bridged complexes $[L^1Co^{III}NCFe^{III}(CN)_5]\cdot 4H_2O$ (L^1 = 6-methyl-1,4,8,11-tetraazacyclotetra-decan-6-amine; 1.941(8) Å) and $[L^2Co^{III}NCFe^{III}(CN)_5]\cdot 4H_2O$ (L^2 = 10-methyl-1,4,8,12-tetraazacyclopentadecan-10-amine; 1.897(14) Å),[8] which is in agreement with the presence of high-spin cobalt(II) ions. The Co-N≡C entities in **1** (165.8(2) and 169.4(2)°) and **2** (164.77(2)

---

[*] Prof. Dr. M. Julve, Dr. R. Lescouëzec, Prof. Dr. F. Lloret, Dr. R. Carrasco
Departament de Química Inorgànica/Instituto de Ciencia Molecular
Facultat de Química de la Universitat de València
Dr. Moliner 50, 46100 Burjassot, València (Spain)
Fax: (+34) 96-386-4322
E-mail: miguel.julve@uv.es

Prof. Dr. M. Verdaguer, Dr. J. Vaissermann, Dr. Y. Dromzee
Laboratoire de Chimie Inorganique et Matériaux Moléculaires
Unité CNRS 7071, Université Pierre et Marie Curie
4 Place Jussieu, Case 42, 75252 Paris Cedex 05 (France)
Fax: (+33) 1-4427-3841
E-mail: miv@ccr.jussieu.fr

Prof. Dr. C. Ruiz-Pérez
Laboratorio de Rayos X y Materiales Moleculares
Departamento de Física Fundamental II
Facultad de Física de la Universidad de La Laguna
Avda. Astrofísico Francisco Sánchez s/n, 38204 La Laguna, Tenerife (Spain)

Prof. Dr. D. Gatteschi
Dipartimento di Chimica
Università degli Studi di Firenze
Via della Lastruccia, 3, 50019 Sesto Fiorentino (FI) (Italy)

Dr. W. Wernsdorfer
Laboratoire Louis Néel, C.N.R.S.
BP 166, 25 Avenue des Martyrs, 38042 Grenoble Cedex 9 (France)

[**] This work was supported by the TMR Programme from the European Union (contract ERBFM-RXCT98-0181), the Spanish Ministry of Science and Technology (project BQU2001-2928), the French Ministry of National Education and the European Science Foundation through the Molecular Magnets Programme.

Supporting information for this article is available on the WWW under http://www.angewandte.org or from the author.

DOI: 10.1002/ange.200250243

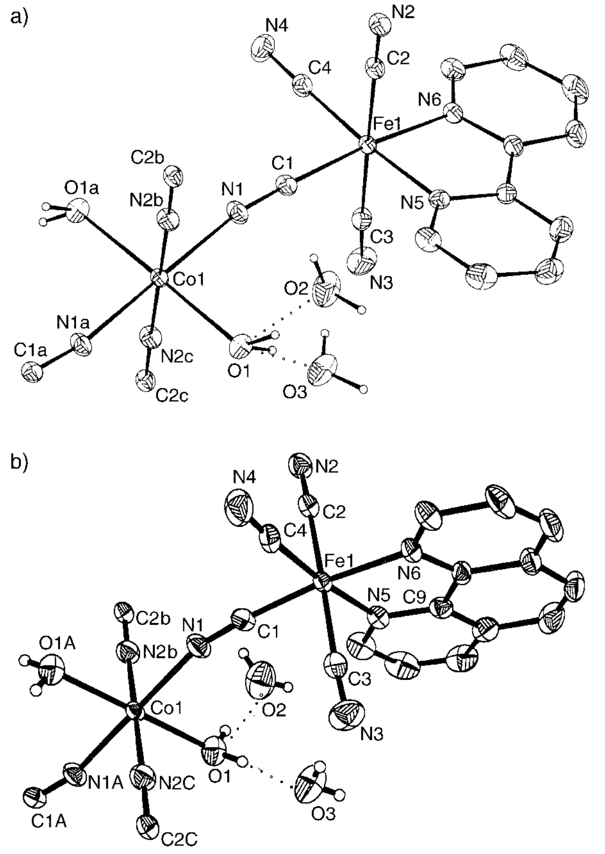

Figure 1. Perspective view of the crystallographically independent unit of **1** (a) and **2** (b), thermal ellipsoids set at 30% probability and hydrogen atoms of bpy omitted for clarity. The hydrogen bonds involving the water molecules are illustrated by broken lines. Selected bond lengths [Å] and angles [°] for compounds **1**/**2**: Fe1-C1 1.923(3)/1.925(3), Fe1-C2 1.951(2)/1.950(2), Fe1-C3 1.949(3)/1.954(2), Fe1-C4 1.909(3)/1.912(3), Fe1-N5 1.980(2)/1.999(2), Fe1-N6 1.991(2)/1.999(2), Co1-N1 2.125(2)/2.147(2), Co1-N2b 2.104(2)/2.113(2), Co1-O1 2.103(2)/2.089(2); N5-Fe1-N6 81.23(9)/81.86(8), N1-Co1-N2b 88.00(9)/90.55(8). See text for further details.

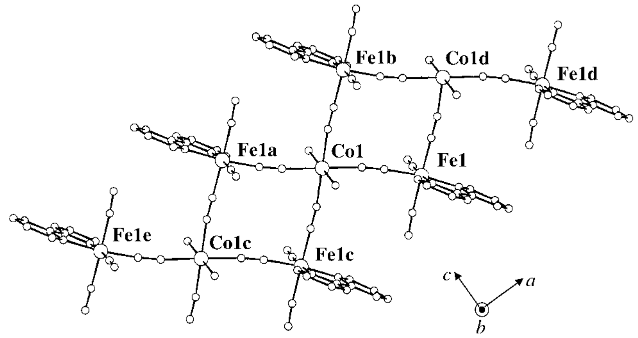

Figure 2. Perspective view of a fragment of the double zigzag chain of **1** running parallel to the *a* axis. The uncoordinated water molecules have been omitted for clarity. Symmetry codes: (a) $-x, 1-y, -z$; (b) $1-x, 1-y, -z$; (c) $-1+x, y, z$; (d) $1+x, y, z$; (e) $-1-x, 1-y, -z$.

and 165.37(1)°) are significantly bent. The shortest interchain metal–metal distances are 7.595(1) (**1**) and 7.656(1) Å (**2**) [Fe(1)···Co(1f); (f) = $1/2-x$, $1/2+y$, $-1/2-z$] and 8.372(1) (**1**) and 9.856(2) Å (**2**) [Fe(1)···Fe(1f)].

At room temperature, the $\chi_M T$ product for powder samples of **1** and **2** (χ_M is the magnetic susceptibility per Fe_2Co unit) is 4.4 and 3.9 cm^{3}mol^{-1}K, respectively (Figure S1 and S2 in the Supporting Information), and corresponds to the presence of one high-spin Co^{II} ($S_{Co} = 3/2$) and two low-spin Fe^{III} ($S_{Fe} = 1/2$) ions, with significant orbital contributions. Upon cooling under an applied magnetic field of 100 Oe, $\chi_M T$ increases linearly, in line with an intrachain ferromagnetic coupling between Fe^{III} and Co^{II} centers. The increase is smooth in the high-temperature range and sharp at $T < 50$ K. $\chi_M T$ reaches a maximum value of about 460 cm^{3}mol^{-1}K (**1** and **2**) at 7.5 K and further decreases linearly with T (as the magnetization becomes field dependent). Below 8 K, hysteresis loops as well as maxima of the in-phase and out-of-phase signals which are strongly frequency dependent are observed for both compounds. In this temperature range, a thermally activated mechanism appears to be involved. Such a behavior has been observed in superparamagnets,[9] spin glasses,[10] molecular anisotropic high-spin clusters,[11] and in the anisotropic chain reported in ref. [1]. To characterize the anisotropy of **1** and **2**, we performed magnetization measurements on single crystals. For complex **1** the main results are summarized in Figures 3, 5, and 6 (similar behavior is observed for **2**). The static magnetization was measured under an applied magnetic field (Figure 3). The magnetization along the *b* axis ($\alpha = 90$ or 270°) is greater than that along the *c* axis ($\alpha = 0$ or 180°). Minima of the magnetization are observed at ±59° with respect to the *b* axis ($\alpha = 31$ or 149°). These features indicate that each chain within the crystal presents an easy magnetization axis along the Co–O$_{water}$ bond. These compounds have two chains, the Co–O$_{water}$ bonds of which make an angle of ±31° with the *b* axis, and this bond defines the direction of the easy magnetization axis for each chain (see Figure 4). So, the magnetization along any direction ($M\alpha$) in the *bc* plane would correspond to the sum of these vectors (noted m_1 and m_2 in Figure 4) through Equation (1).

$$M\alpha = m_1 \cos\alpha + m_2 \cos(\alpha + 62) \qquad (1)$$

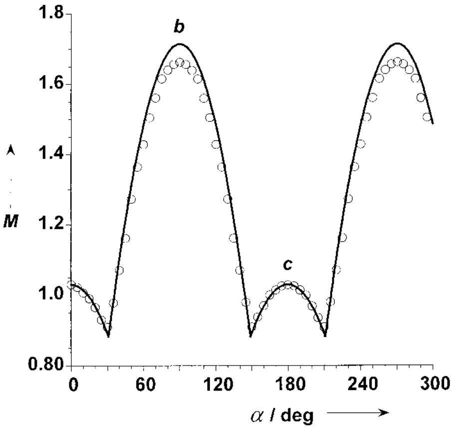

Figure 3. Dependence of the magnetization *M* (arbitrary units) of a single crystal of **1** versus the rotation angle *α* in the *bc* plane and under an applied magnetic field *H* of 5000 Oe at 5 K. The 0 and 90° angles correspond to $H \parallel c$ and $H \parallel b$, respectively: (○) experimental data; (——) theoretical data obtained from Equation (1) (see text).

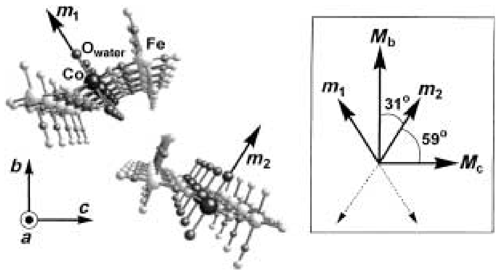

Figure 4. Orientation of the vectors of the double-chain structure.

This equation reproduces the experimental data in Figure 3. The magnetization is greater along the *b* axis than along the *c* axis because the m_1 and m_2 vectors make a smaller angle with the *b* axis than the *c* axis (31° at *b* versus 59° at *c*). The magnetization minima are observed when the magnetic field is perpendicular to one of the two vectors (that is ±59° with respect to *b*).

The magnetization along the *a* axis is very weak (Figure 5). This can be understood taking into account that the chains run parallel to the *a* axis, and consequently, the m_1 and m_2 vectors are practically perpendicular to this axis (they form an angle of 89°). All these features demonstrate the anisotropic, Ising-type behavior of each of the two chains.

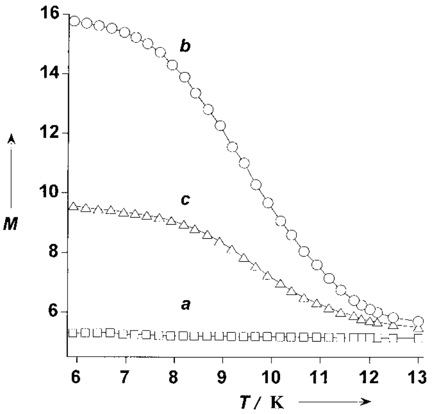

Figure 5. Field-cooled magnetization (FCM) of a single crystal of **1** along the *a*, *b*, and *c* axes, with an external field of 1000 Oe.

They are in agreement with the results obtained on a micro SQUID (superconducting quantum-interference device) applying a transversal magnetic field.

The value of the coercive field (H_c) of the hysteresis loop for a single crystal of **1** is strongly dependent on the temperature and the sweep rate. So, for $H \parallel b$, H_c increases from 1000 to 12000 Oe when going from 2 to 1.1 K at 0.002 $\mathrm{T\,s^{-1}}$ whereas it decreases when increasing the sweep rate (5000 and 750 Oe when going from 0.07 to 0.001 $\mathrm{T\,s^{-1}}$ at $T = 2$ K) (Figure S4 and S5, Supporting Information).

The ac measurements along the *b* axis show a frequency dependence (Figure 6), and the relaxation time of the magnetization (τ, not shown) presents an exponential behavior [$\tau = \tau_0 \exp(E_a/kT)$] in the frequency range explored (0.1–1000 Hz). The best-fit parameters for **1** are $\tau_0 = 9.4 \times 10^{-12}$ s; $E_a/k_B = 142$ K.

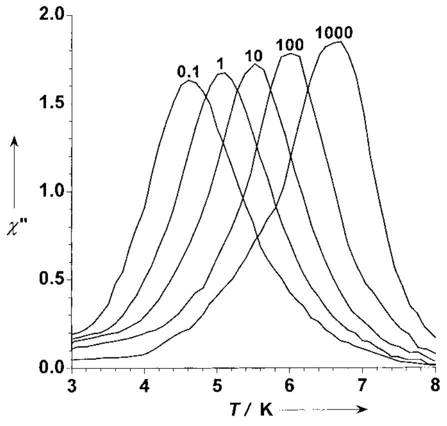

Figure 6. Temperature dependence of the out-of-phase (χ'') component of the ac susceptibility on a single crystal of **1** in zero applied static field and with the oscillating field (1 Oe) applied along the *b* axis. The values of the frequency of the oscillating field are 1000, 100, 10, 1, and 0.1 Hz.

All these magnetic data clearly do not correspond to a 3D-ordered system. In fact, heat-capacity measurements on single crystals of **1** (Figure S3, Supporting Information) do not show any λ peak down to 1.8 K. A spin-glass system would have presented similar ac behavior but the hypothesis can be discarded since the measurements were carried out on well organized single crystals. We are left with the presence of a slow relaxation of the magnetization in these two new 1D compounds. These compounds are reminiscent of the mixed radical cobalt(II) chain in ref. [1]. The chains **1** and **2** are 1D Ising systems, and fulfill the conditions required to observe slow relaxation of the magnetization. In summary, the double-chain topology, the bimetallic character with two anisotropic spin bearers, and the ferromagnetic coupling in **1** and **2** lead to the observation of a slow relaxation of the magnetization and to original properties which deserve more theoretical and experimental studies on pure and doped systems.

The lack of an appropriate analytical expression of the magnetic susceptibility impedes the evaluation of the ferromagnetic *J* constant. Nevertheless, it is possible to understand qualitatively the ferromagnetic nature of the coupling between low-spin $\mathrm{Fe^{III}}$ and high-spin $\mathrm{Co^{II}}$ centers in **1** and **2** thanks to DFT calculations. They show that in a local octahedral symmetry, the three unpaired electrons on the cobalt center are in d_{z^2}, $d_{x^2-y^2}$, and d_{xy} orbitals (*z* axis along the $\mathrm{Co{-}O_{water}}$ bonds and *x* and *y* axes along the Co-N≡C(cyanide) bonds) whereas that of the iron atom is in a mixture of d_{xy} and d_{xz} orbitals (keeping the same reference axes). The situation corresponds to a predominant orthogonality between the two sets of orbitals on the cobalt and iron centers and accounts for the observed ferromagnetic coupling.

Experimental Section

1: Red rodlike single crystals of **1** were obtained by slow diffusion of aqueous solutions of $\mathrm{Li[Fe(bpy)(CN)_4]}$ (isolated by metathetic reaction of $\mathrm{PPh_4[Fe(bpy)(CN)_4]\cdot H_2O}$ and $\mathrm{LiClO_4}$ in a 1:1 molar ratio in acetonitrile) and $\mathrm{[Co(H_2O)_6](NO_3)_2}$ in an H-shaped tube in the dark. In a typical experiment, aqueous solutions of the iron salt (0.2 mmol) in one arm and of the cobalt salt (0.1 mmol) in the other one were allowed to diffuse in the dark. X-ray quality single crystals of **1** were formed in the iron-containing arm after a few weeks, the yield being practically quantitative. When the experiment was carried out in day light, the yield was very low because of the precipitation of an insoluble green solid $[\{Fe^{II}(bpy)(CN)_4\}_3Co^{III}_2]$ as the main product. Elemental analysis (C, H, N) and the Fe:Co molar ratio (electron microscopy) on crystals of **1** agree well with its formulation as a tetrahydrate. IR (KBr disk) of **1**: $\tilde{\nu} = \nu_{CN}$ 2167w and 2156m (bridging cyanide) and 2124s cm^{-1} (terminal cyanide).

2: Purple-red platelike single crystals of **2** were obtained by following the procedure described for **1** but using the $PPh_4[Fe(phen)(CN)_4]\cdot 2H_2O$ complex as the iron precursor. The yield was also quantitative when working in the dark. Elemental analysis (C, H, N) and the Fe:Co molar ratio (electron microscopy) on crystals of **2** agree well with its formulation as a tetrahydrate. IR (KBr disk) of **2**: $\tilde{\nu} = \nu_{CN}$ 2165w and 2155m (bridging cyanide) and 2123s cm^{-1} (terminal cyanide).

Received: September 25, 2002 [Z50243]

Keywords: chain structures · cobalt · cyanide ligands · ferromagnetism · iron

---

[1] A. Caneschi, D. Gatteschi, N. Lalioti, C. Sangregorio, R. Sessoli, G. Venturi, A. Vindigni, A. Rettori, M. G. Pini, M. A. Novak, *Angew. Chem.* **2001**, *113*, 1810; *Angew. Chem. Int. Ed.* **2001**, *40*, 1760.

[2] R. J. Glauber, *J. Math. Phys.* **1963**, *4*, 294.

[3] R. Lescouëzec, PhD Thesis, Valencia and Paris, **2002**.

[4] R. Lescouëzec, F. Lloret, M. Julve, J. Vaissermann, M. Verdaguer, R. Llusar, S. Uriel, *Inorg. Chem.* **2001**, *40*, 2065.

[5] R. Lescouëzec, F. Lloret, M. Julve, J. Vaissermann, M. Verdaguer, *Inorg. Chem.* **2002**, *41*, 818.

[6] Crystal data: compound **1**: $C_{28}H_{28}CoFe_2N_{12}O_6$, $M_r = 799.2$, monoclinic, space group $P2_1/n$, $a = 7.592(1)$, $b = 15.190(7)$, $c = 14.714(3)$ Å, $\beta = 92.92(1)°$, $V = 1694.6(9)$ Å^3, $Z = 2$, $\rho_{calcd} = 1.57$ g cm^{-3}, $\lambda = 0.71069$ Å, $\mu(Mo_{K\alpha}) = 13.8$ cm^{-1}, $F(000) = 816$, GoF = 1.04. A total of 3354 reflections were collected and 2972 are unique ($R_{int} = 0.02$). $R1$ and $wR2$ are 0.0342 and 0.0401, respectively, for 224 parameters and 2546 reflections [$I > 3\sigma(I)$]. Compound **2**: $C_{32}H_{28}CoFe_2N_{12}O_6$, $M_r = 847.29$, monoclinic, space group $P2_1/n$, $a = 7.4315(18)$, $b = 15.614(4)$, $c = 15.344(4)$ Å, $\beta = 93.444(6)°$, $V = 1777.3(7)$ Å^3, $Z = 2$, $\rho_{calcd} = 1.583$ g cm^{-3}, $\lambda = 0.71073$ Å, $\mu(Mo_{K\alpha}) = 13.29$ cm^{-1}, $F(000) = 862$, GoF = 0.890. A total of 14566 reflections were collected and 5316 are unique ($R_{int} = 0.054$). $R1$ and $wR2$ are 0.0396 and 0.0823, respectively, for 298 parameters and 3318 reflections [$I > 2\sigma(I)$]. The data were collected on Enraf-Nonius MACH-3 (**1**) and Bruker Smart CCD (**2**) diffractometers with $Mo_{K\alpha}$ radiation at 295 K. The structures were solved by direct methods through the SHELX-86 (**1**) and SHELX-97 (**2**) programs and refined with full-matrix least-squares technique on F (**1**) and F^2 (**2**) through the PC version of CRYSTALS (**1**) and the SHELXL-97 (**2**) program. All non-hydrogen atoms were refined anisotropically. CCDC-191049 (**1**) and CCDC-191050 (**2**) contain the supplementary crystallographic data for this paper. These data can be obtained free of charge via www.ccdc.cam.ac.uk/conts/retrieving.html (or from the Cambridge Crystallographic Data Centre, 12, Union Road, Cambridge CB21EZ, UK; fax: (+44)1223-336-033; or deposit@ccdc.cam.ac.uk).

[7] G. De Munno, M. Julve, F. Lloret, J. Faus, A. Caneschi, *J. Chem. Soc. Dalton Trans.* **1994**, 1175; J. Brunzelle, A. Fitch, Y. Wang, S. F. Pavkovic, *Acta Crystallogr. Sect. C* **1996**, *52*, 2984.

[8] P. V. Bernhardt, B. P. Macpherson, M. Martínez, *Inorg. Chem.* **2000**, *39*, 5203.

[9] A. H. Morrish, *The Physical Principles of Magnetism*, Wiley, New York, **1966**.

[10] J. A. Mydosh, *Spin Glasses: An Experimental Introduction*, Taylor&Francis, London, **1993**.

[11] a) R. Sessoli, D. Gatteschi, A. Caneschi, M. A. Novak, *Nature* **1993**, *365*, 141; b) L. Thomas, F. Lionti, R. Ballou, D. Gatteschi, R. Sessoli, B. Barbara, *Nature* **1996**, *383*, 145; c) W. Wernsdorfer, R. Sessoli, *Science* **1999**, *284*, 133.